Heralded processes on continuous-variable spaces as quantum maps

Franck Ferreyrol,[1,2] Nicolò Spagnolo,[1,3] Rémi Blandino,[1] Marco Barbieri,[1,4] and Rosa Tualle-Brouri[1,5]

[1]*Laboratoire Charles Fabry, Institut d'Optique, Université Paris-Sud and CNRS, F-91127 Palaiseau, France*
[2]*Centre for Quantum Dynamics and Centre for Quantum Computation and Communication Technology, Griffith University, Brisbane 4111, Australia*
[3]*Dipartimento di Fisica, Sapienza Università di Roma, Piazzale Aldo Moro 5, I-00185 Rome, Italy*
[4]*Clarendon Laboratory, Department of Physics, University of Oxford, Oxford OX1 3PU, United Kingdom*
[5]*Institut Universitaire de France, 103 Boulevard St. Michel, 75005 Paris, France*

Conditional evolution is crucial for generating non-Gaussian resources for quantum-information tasks in the continuous variable scenario. However, tools are lacking for a convenient representation of heralded processes in terms of quantum maps for continuous variable states, in the same way as Wigner functions are able to give a compact description of the quantum state. Here we propose and study such a representation, based on the introduction of a suitable transfer function to describe the action of a quantum operation on a Wigner function. We also reconstruct the maps of two relevant examples of conditional processes, that is, noiseless amplification and photon addition, by combining experimental data and a detailed physical model. This analysis allows us to fully characterize the effect of experimental imperfections in their implementations.

PACS number(s): 03.67.Ac, 03.65.−w

I. INTRODUCTION

Quantum mechanics is a probabilistic theory. The quantum description of any experiment is based on probability amplitudes—quantum states and measurements—and transformations of such amplitudes—quantum processes. For each of these objects there exist techniques to obtain the corresponding mathematical tool from measured data: state tomography [1,2], process tomography [3,4], and detector tomography [5]. There exist constraints necessary to attribute a near physical meaning to abstract mathematics: for instance, a map acting on density matrices' space corresponding to a physical process is normally completely positive (CP). This amounts to saying that it must send physical states into physical states regardless of observing the system by itself or as a part of a larger ensemble to which it is decoupled [6]. Most of the studied maps preserve the norm of the state, but there exist notable exceptions: non-trace-preserving operations arise whenever a measurement on the system is involved.

An interesting class of such processes involves heralding: the evolution of a system is considered conditionally on the outcome of a measurement on part of the system itself [7] (see Fig. 1). In the context of optical quantum information, conditional evolution has found several applications for simulating strong nonlinearities at the few-photon level. This approach has allowed researchers to build two-qubit [3] and three-qubit quantum logic gates [8] and to generate quantum states with non-Gaussian Wigner functions [9–13]. Such an evolution is able to induce non-Gaussian transformations effective in overcoming existing no-go theorems valid for purely Gaussian resources [14–16]. Successful applications of such processes to communication tasks have been demonstrated in several experiments [17–20].

The experimental investigation is relatively at an early stage: so far quantum process tomography of non-trace-preserving maps has been implemented only in a reduced two-qubit Hilbert space [21,22]. Here we show, by a detailed physical model, the description of two conditioned processes

which are relevant to continuous-variable state manipulation: the noiseless amplifier [19,20] and the single-photon addition [11,23]. We can derive the expression of the map in the well-known tensor form, and, as a step further, we illustrate a transfer function formalism, which allows us to describe the quantum process directly in the Wigner representation. This will stimulate more in-depth investigation in this area and the development of more sophisticated analytic tools.

II. QUANTUM MAPS

Any transformation acting on states needs to satisfy some physically motivated mathematical constraints. In the simplest case, a closed system, the evolution of a quantum state is described by a unitary operator, $\hat{U}$, which transforms the input state as $\rho' = \hat{U}\rho\hat{U}^{\dagger}$. More generally, the system will be able to interact with the environment and a representation in terms of a unitary operator won't be sufficient to describe this scenario; however, some essential features are retained, in particular, the output state must be obtained from a linear transformation of the input. The proper formalism then adopts a generic linear map, $\mathcal{E}$, such that $\rho' = \mathcal{E}(\rho)$. Similarly to the previous expression, this map can be decomposed in the incoherent application of a set of Kraus operators $\{\hat{E}_i\}$ [6]:

$$\mathcal{E}(\rho) = \sum_i \hat{E}_i \rho \hat{E}_i^{\dagger}, \tag{1}$$

with, for deterministic processes,

$$\sum_i \hat{E}_i \hat{E}_i^{\dagger} = \mathbb{1}. \tag{2}$$

One can note that this expression is similar to the formalism used for a positive-operator-valued measure (POVM) since a generic transformation can be seen as the application of a unitary operation on a system composed by the input state and the environment, followed by a measurement of the environment for which we do not know the outcome. Another

expression, more convenient for data visualization, uses the tensor $\{\mathcal{E}_{l,k}^{n,m}\}$:

$$[\mathcal{E}(\varrho)]_{l,k} = \sum_{n,m} \mathcal{E}_{l,k}^{n,m} \varrho_{n,m}, \qquad (3)$$

where the elements of the tensor are given by $\mathcal{E}_{l,k}^{n,m} = \sum_i \langle l|\hat{E}_i|n\rangle\langle m|\hat{E}_i^\dagger|k\rangle$.

These maps cannot be completely arbitrary: an essential requirement is that they lead physical states into physical states. Therefore, these maps have to send positive operators into positive operators and, for deterministic processes, are required to preserve the trace; so they directly give a physical density matrix without the need for other operations. Furthermore, in the majority of the cases, we also demand complete positiveness: this amounts to saying that the evolution must remain physical when the system is entangled with a second object.

A somewhat different context arises when considering a conditional process: it implies a nonlinear evolution of the state due to the renormalization operation. Indeed, these processes often aim to approximate a nonunitary and nonphysical—i.e., trace increasing—linear operator $\hat{C}$ and transform a pure state $|\alpha\rangle$ into $\sqrt{N(\alpha)}\hat{C}|\alpha\rangle$, where $N(\alpha)$ is the normalization factor, which might present a complex dependence on the state. Even if $\hat{C}$ is actually linear, this linearity is hidden if we consider the physical inputs, as $\sqrt{N(\alpha)}\hat{C}|\alpha\rangle + \sqrt{N(\beta)}\hat{C}|\beta\rangle \neq \sqrt{N(\alpha+\beta)}\hat{C}(|\alpha\rangle + |\beta\rangle)$. As a result, in order to represent it as a linear quantum map one should use a non-trace-preserving map and keep the normalization step for the result of the process. Moreover, a map should include one more piece of information to describe a conditional process: the success probability.

In fact, a conditional evolution acts as follows: the system evolves through a probabilistic device, and we only accept those runs when a successful event is flagged (Fig. 1). Clearly, the overall process including both successes and failures can be modeled by a deterministic quantum map. In terms of Kraus decomposition [Eq. (3)] passage from the overall process to the
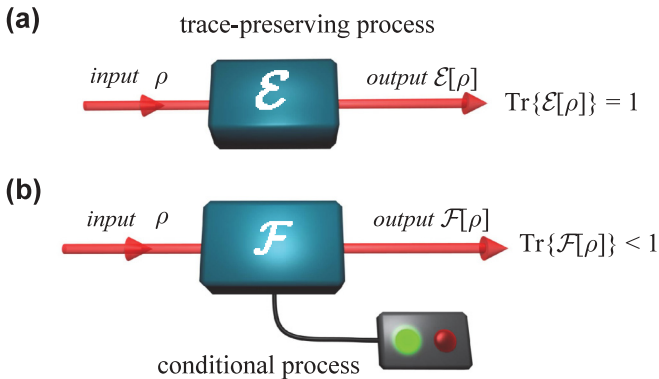
(a) trace-preserving process

(b)

FIG. 1. (Color online) (a) Trace-preserving quantum operation. The input state ϱ is transformed by the quantum channel $\mathcal{E}$ in the output state $\mathcal{E}[\varrho]$. The trace of the input state is preserved by the channel: $\mathrm{Tr}\{\mathcal{E}[\varrho]\} = 1$. (b) Heralded quantum operation. The input state ϱ is transformed by the quantum channel $\mathcal{F}$ in the output state $\mathcal{F}[\varrho]$ upon realization of a conditional event. The trace of the input state is, in general, not preserved by the channel: $\mathrm{Tr}\{\mathcal{F}[\varrho]\} < 1$.

conditional one consists in keeping only the subset of the Kraus operators corresponding to the result of the measure used for heralding. Thus we easily see that the trace of the output state gives our additional information: the success probability, and a quantum map only needs to be non-trace-increasing to correspond to a physical operation [24].

The method explained above gives a neat picture of the process for discrete-variable systems: for instance, one can recognize almost at glance the behavior of a qubit process by inspecting the corresponding tensor. This is more complex when dealing with continuous-variable systems, when often looking at the states as Wigner quasi-distribution in the phase space can convey information in a more compact and effective way. Therefore, a method to represent quantum processes in the Wigner representation would be highly desirable. Such an object has been proposed for the unitary processes [25,26] and for Gaussian operations [15] and has similarities with time evolution approaches based on differential equations [27]; here we give an explicit extension of these results to the case of a generic map, $\mathcal{E}$.

For this purpose, we can reason in analogy with the probability distribution $\mathcal{P}(x,p)$ for physical position and momentum of a classical particle. The action of a Markovian process will modify such distribution via a transfer function $f(x',p',x,p)$, describing the odds that a particle initially in the position (x,p) will eventually end in (x',p'). The distribution $\mathcal{P}'(x',p')$ of the coordinates at the end of the process will result from the sum of all these elementary displacements:

$$\mathcal{P}'(x',p') = \int dx\,dp\,\mathcal{P}(x,p)f(x',p',x,p). \qquad (4)$$

Hence, we would like to maintain this structure for quantum processes as well by introducing a suitable transfer function, $f_{\mathcal{E}}(x',p',x,p)$, by which the input Wigner function $W(x,p)$ can be turned into the output $W'(x',p')$ by the integral transform:

$$W'(x',p') = \int dx\,dp\,W(x,p)f_{\mathcal{E}}(x',p',x,p). \qquad (5)$$

In order to see that this is actually the case, we start from the case where only one Kraus operator $\hat{E}_i$ is present; the general result can be obtain by linearity. The Wigner function of the output state then reads

$$W'(x',p') = \frac{1}{2\pi}\int d\nu\,e^{i\nu p'}\left\langle x' - \frac{\nu}{2}\left|\hat{E}_i\rho\hat{E}_i^\dagger\right|x' + \frac{\nu}{2}\right\rangle. \qquad (6)$$

We invoke the completeness relation $\int |s\rangle\langle s|ds = 1$ and the formula $\langle s|E|t\rangle = \int e^{i(s-t)p}W(\frac{s+t}{2},p)dp$ to obtain

$$W'(x',p') = \frac{1}{2\pi}\int dp\,d\nu\,ds\,dt\,e^{i\nu p'}e^{i(s-t)p}W\left(\frac{s+t}{2},p\right)$$
$$\times\left\langle x' - \frac{\nu}{2}\left|\hat{E}_i\right|s\right\rangle\langle t|\hat{E}_i^\dagger\left|x' + \frac{\nu}{2}\right\rangle, \qquad (7)$$

and then, by a variable substitution, the expression for the transfer function associated to the operator $\hat{E}_i$:

$$f_i(x',p',x,p) = \frac{1}{2\pi}\int d\mu\,d\nu\,e^{i\nu p'}e^{i\mu p}\left\langle x' - \frac{\nu}{2}\left|\hat{E}_i\right|x + \frac{\mu}{2}\right\rangle$$
$$\times\left\langle x - \frac{\mu}{2}\left|\hat{E}_i^\dagger\right|x' + \frac{\nu}{2}\right\rangle, \qquad (8)$$

which implies

$$\int f_i(x',p',x,p)dx'dp' = W_{\hat{E}_i^\dagger \hat{E}_i}(x,p), \qquad (9)$$

$$\int f_i(x',p',x,p)dxdp = W_{\hat{E}_i \hat{E}_i^\dagger}(x',p'). \qquad (10)$$

Based on the remark that each $\hat{E}_i$ acts independently, the transfer function associated with a generic process reads

$$f_{\mathcal{E}}(x',p',x,p) = \sum_i f_i(x',p',x,p), \qquad (11)$$

where each function f_i corresponds to a Kraus operator with the relation given by Eq. (8). It can be checked that using this formula as the definition, and using the relation between $\mathcal{E}_{l,k}^{n,m}$ and $\hat{E}_i$, one arrives at the original definition. The transfer function might be a distribution, but from Eq. (8) it appears that it is always real. Also, normalization enforces that

$$\int f_i(x',p',x,p)dx'dp'dxdp = \mathrm{Tr}(\hat{E}_i^\dagger \hat{E}_i) \qquad (12)$$

$$= \mathrm{Tr}(\hat{E}_i \hat{E}_i^\dagger). \qquad (13)$$

Those properties can easily be extended to the whole transfer function. In particular, in the case of a deterministic map we have

$$\int f_i(x',p',x,p)dx'dp' = 1, \qquad (14)$$

whereas for a nondeterministic process the integral of $W_{\hat{E}_i^\dagger \hat{E}_i}(x,p)W(x,p)$ gives the success probability.

We also can express the transfer function in terms of the process tensor, starting with Eq. (3) rewritten in the form

$$\mathcal{E}(\varrho) = \sum_{n,m}\sum_{l,k} \mathcal{E}_{l,k}^{n,m}\mathrm{Tr}(\varrho|n\rangle\langle m|)|l\rangle\langle k|. \qquad (15)$$

We can use the properties of the Wigner functions to evaluate the expectation value $\mathrm{Tr}(\varrho|n\rangle\langle m|)$ and derive

$$W'(x',p') = 2\pi \int dx\,dp\,W(x,p)$$
$$\times \left(\sum_{m,n}\sum_{l,k} \mathcal{E}_{l,k}^{n,m} W_{|n\rangle\langle m|}(x,p)W_{|l\rangle\langle k|}(x',p') \right), \qquad (16)$$

where $W_{|l\rangle\langle k|}(x,p)$ is the Wigner representation of $|l\rangle\langle k|$. Therefore, the quantum operation $\mathcal{E}$ is conveniently represented by the transfer function

$$f_{\mathcal{E}}(x',p',x,p) = 2\pi \sum_{n,m}\sum_{l,k} \mathcal{E}_{l,k}^{n,m} W_{|n\rangle\langle m|}(x,p)W_{|l\rangle\langle k|}(x',p'). \qquad (17)$$

From this equation one can also easily derive the link between transfer function and other representations as "vectorized" density matrices [28] and Choi-Jamiokowski matrices [29].

The quantum transfer function still bares resemblance to the Markovian processes. This can be seen by inspecting what happens when chaining two processes: $\mathcal{E} = \mathcal{E}_1 \circ \mathcal{E}_2$. Under these circumstances, we obtain the complete transfer

function as

$$f_{\mathcal{E}}(x',p',x,p) = \int dx''\,dp''f_{\mathcal{E}_2}(x',p',x'',p'')f_{\mathcal{E}_1}(x'',p'',x,p), \qquad (18)$$

which is similar to the Chapman-Kolmogorov equation for Markovian processes [26]. This reinforces the view that, from a classical viewpoint, $f_{\mathcal{E}}(x',p',x,p)$ should be interpreted as a transition probability from $\{x,p\}$ to $\{x',p'\}$. The analogy cannot be extended further in the quantum domain: in the following, we illustrate a case where $f_{\mathcal{E}}(x',p',x,p)$ can actually take negative values. As for the Wigner function [30,31], this negativity is linked to nonclassicality. However, we also show how the temptation to transform those links into a direct quantitative connection has to be resisted.

One can note that such a definition uses very few assumptions about the transformation and so can be extended to more general processes, as long as the transformation remains linear in the quantum state. In particular, as for the tensor form [32], it can be used with trace-increasing maps, which, even if they are not physical, are very common in theoretical quantum physics and include most of the nonunitary operators that are approximated by conditional processes.

III. DETERMINATION OF THE TRANSFER FUNCTION

In order to determine the expression of the transfer function, one could first decompose it in a sum of transfer functions corresponding to the different heralding events, in a way similar to Eq. (11). Then, each of those transfer functions can be constructed by composing, with the use of Eq. (18), some basic transfer functions corresponding to the different elements of the process. The basic transfer functions can have the same number of input and output modes, corresponding to a basic transformation; only output modes, corresponding to the introduction of an ancilla state; or only input modes, corresponding to a measurement.

The basic transformations can be determined by Eq. (8) or by simple considerations. In particular all transformations that can be expressed as coordinate transformations have transfer functions composed of Dirac distributions which directly come from the coordinate transformation. Another interesting basic transformation is the one given by a coordinate transformation M_i ($i = x,p$) for each quadrature of the input mode and a quadrature of a vacuum ancilla, followed by a partial trace on the ancilla. If the transformation matrix is

$$M_i = \begin{pmatrix} \mu_i & \nu_i \\ \varepsilon\nu_i & \mu_i \end{pmatrix}, \qquad (19)$$

$$\det(M_i) = 1, \qquad (20)$$

where $\varepsilon = \pm 1$, then the transfer function of this operation is

$$f(x',p',x,p) = \frac{\nu_x\nu_p}{\pi} \exp\left[-\left(\frac{x' - \mu_x x}{\nu_x}\right)^2 \right]$$
$$\times \exp\left[-\left(\frac{p' - \mu_p p}{\nu_p}\right)^2 \right]. \qquad (21)$$

Table I shows some basics transfer functions obtained by those considerations with their tensor form.

TABLE I. Tensor process and transfer functions of some basic transformations.

Transformation	Tensor (see [32])	Transfer function
Identity	$\delta_{k,n}\delta_{l,m}$	$\delta(x-x')\delta(p-p')$
Phase rotation	$e^{\theta(k-l)}\delta_{k,n}\delta_{l,m}$	$\delta(x-\cos\theta x'+\sin\theta p')\delta(p-\cos\theta p'-\sin\theta x')$
Displacement	$\sqrt{m!n!l!k!}e^{|\alpha|^2}\sum_{i=0}^{m}\sum_{j=0}^{n} n\binom{m}{i}\binom{n}{j}$	$\delta(x-x'+\sqrt{2}\mathrm{Re}(\alpha))\delta(p-p'+\sqrt{2}\mathrm{Im}(\alpha))$
	$\frac{(-1)^{m+n-i-j}}{(l-i)!(k-j)!}\alpha^{l+n-i-j}\bar{\alpha}^{k+m-i-j}$	
Squeezing	$\frac{\sqrt{k!l!}}{(m!n!0^{3/2}}\cosh(r)^{k+l-1}\sum_{i=o}^{k}\sum_{j=0}^{l}2^{i+j}$ $\times\frac{\sqrt{(n+k-2i)!(l+m-2j)!}}{\left(\frac{n+k}{2}-i\right)!\left(\frac{m+l}{2}-j\right)!}\left(-\frac{\tanh(r)}{2}\right)^{(m+n+l+k)/2}$ $\times\frac{(n+k-i)!}{i!(k-i)!}\frac{(m+l-j)!}{k!(l-j)!}\frac{1+(-1)^{n+k}}{2}\frac{1+(-1)^{m+l}}{2}$	$\delta(x-e^r x')\delta(p-e^{-r}p')$
Beam splitter	$\sqrt{\frac{m_1!m_2!n_1!n_2!}{l_1!l_2!k_1!k_2!}}\sum_{i=0}^{l_1}\sum_{j=0}^{k_1}(-1)^{l_1+k_1-i-j}$ $\times\binom{l_1}{i}\binom{l_2}{m_1-i}\binom{k_1}{j}\binom{k_2}{n_1-j}$ $\times t^{2i+2j+l_2+k_2-m_1-n_1}r^{l_1+k_1+m_1+n_1-2i-2j}$ $\times\delta_{m_1+m_2,l_1+l_2}\delta_{n_1+n_2,k_1+k_2}$	$\delta(x_1-tx_1'+rx_2')\delta(p_1-tp_1'+rp_2')$ $\times\delta(x_2-tx_2'-rx_1')\delta(p_2-tp_2'-rp_1')$
Parametric down-conversion	$\sqrt{\frac{m_1!m_2!n_1!n_2!}{l_1!l_2!k_1!k_2!}}\frac{(g-1)^{(m_1+n_1)/2}}{g^{(m_1+n_1+l_2+k_2)/2+1}}$ $\times\delta_{n_2-n_1,k_2-k_1}\delta_{m_2-m_1,l_2-l_1}$ $\times\sum_{i=0}^{k_1}\sum_{j=0}^{l_1}\frac{(n_2+i)!(m_2+j)!}{(n_1-k_1+i)!(m_1-l_1+j)!}$ $\times\frac{(-1)^{i+j}g^{k_1+l_1-i-j}(g-1)^{i+j-(k_1+l_1)/2}}{i!(k_1-i)!j!(l_1-j)!}$	$\delta(\sqrt{g}x_1+\sqrt{g-1}x_2-x_1')\delta(\sqrt{g}p_1-\sqrt{g-1}p_2-p_1')$ $\times\delta(\sqrt{g}x_2+\sqrt{g-1}x_1-x_2')\delta(\sqrt{g}p_2-\sqrt{g-1}p_1-p_2')$
Attenuation	$\sqrt{\frac{m!n!}{l!k!}}\frac{\eta^{(l+k)/2}(1-\eta)^{m-l}}{(m-l)!}\delta_{m-l,n-k}$	$\frac{1}{\pi(1-\eta)}\exp\left(-\frac{(x'-\sqrt{\eta}x)^2}{1-\eta}-\frac{(p'-\sqrt{\eta}p)^2}{1-\eta}\right)$
Parametric amplification	$\sqrt{\frac{l!k!2^{n+m}}{n!m!2^{l+k}}}\frac{2^{k-m}}{(k-m)!}\frac{g^{k+(m-n)/2}}{(g+1)^{k+n+1}}\delta_{l-n,k-m}$	$\frac{1}{\pi(g-1)}\exp\left(-\frac{(x'-\sqrt{g}x)^2}{g-1}-\frac{(p'-\sqrt{g}p)^2}{g-1}\right)$

The basic functions with only output or input modes are even simpler to determine. Indeed the first ones are exactly the Wigner function of the introduced ancilla, while the second ones are the Wigner function of the projector corresponding to the measure multiplied by a factor 2π. With those considerations, the transfer function can in fact be seen as an extension of the Wigner function.

Finally, the different heralding events are generally the ideal heralding and the faulty ones. Consider for instance a heralded process when conditioning can be faulty in a certain fraction of the total events. We can call $\mathcal{F}_1$ the correct process and $\mathcal{F}_2$ the failure. The output ϱ_{out} state of the whole process will be a convex combination of

$$\varrho_{\mathrm{out}}=\xi\frac{\mathcal{F}_1(\varrho_{\mathrm{in}})}{P_1}+(1-\xi)\frac{\mathcal{F}_2(\varrho_{\mathrm{in}})}{P_2}, \qquad (22)$$

where $P_{1,2}=\mathrm{Tr}[\mathcal{F}_{1,2}(\varrho_{\mathrm{in}})]$ are the success probabilities used here to normalize the results of both maps. If we notice that $\xi=P_1/(P_1+P_2)$, we can then infer that the transformation which includes both events is given by

$$\varrho_{\mathrm{out}}=\frac{\mathcal{F}_1(\varrho_{\mathrm{in}})+\mathcal{F}_2(\varrho_{\mathrm{in}})}{P_1+P_2}, \qquad (23)$$

where P_1+P_2 is effectively the trace of $\mathcal{F}_1(\varrho_{\mathrm{in}})+\mathcal{F}_2(\varrho_{\mathrm{in}})$. This amounts to saying the correct map is $\mathcal{F}=\mathcal{F}_1+\mathcal{F}_2$, provided that $\mathcal{F}_2$ has the correct occurrence probability. This

last point is the most crucial, and the determination of the good faulty process $\mathcal{F}_2$ can be complicated. The simplicity of the expression is due to the fact that the maps already contain the success probability for the heralding process. Nevertheless we should notice that if the false heralding comes from a noisy mode in the input one should add (at least) a supplementary input mode to the map.

IV. EXAMPLE 1: THE NOISELESS AMPLIFIER

We now inspect two important quantum processes with the formalism of quantum maps: we are able to highlight clear signatures of nonclassicality and observe how they degrade under experimental conditions. As an interesting feature, we are able to capture such nonclassical aspects at a glance. Our analysis first concerns the noiseless amplifier ($\hat{C}=g^{\hat{n}}$, where $\hat{n}$ is the number operator and $g>1$) [19,20]. We do not adopt a "black box" approach, but rather a model of the process is used so as to arrive at a description in term of generalized maps, also in the case when all the imperfections are taken into account.

Our device (Fig. 2) is the teleportation-based amplifier proposed in Ref. [33]: its working principle is to use a nonmaximally entangled resource—a single photon split on an asymmetric beam splitter (A-BS)—to perform the teleportation of a coherent state $|\alpha\rangle$. The analog of the Bell-state
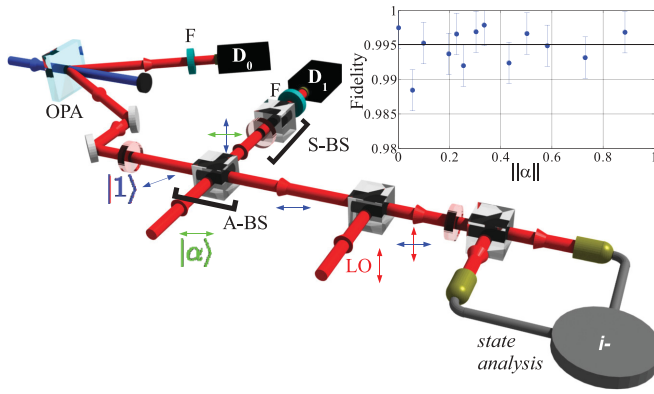
FIG. 2. (Color online) Layout of the implementation of the noiseless amplifier [19]. A single photon is conditionally generated upon detection of a single photon on detector D_0. After splitting in an asymmetric beam-splitter (A-BS), the single photon is mixed with the input coherent state $|\alpha\rangle$ in a symmetric beam-splitter (S-BS). The noiseless amplification process occurs conditionally with the detection of a photon on detector D_1. The beam-splitter operations are performed exploiting polarization (double-sided arrows in the figure). Inset: Fidelities between the experimental density matrices [19] and the prediction of the model.
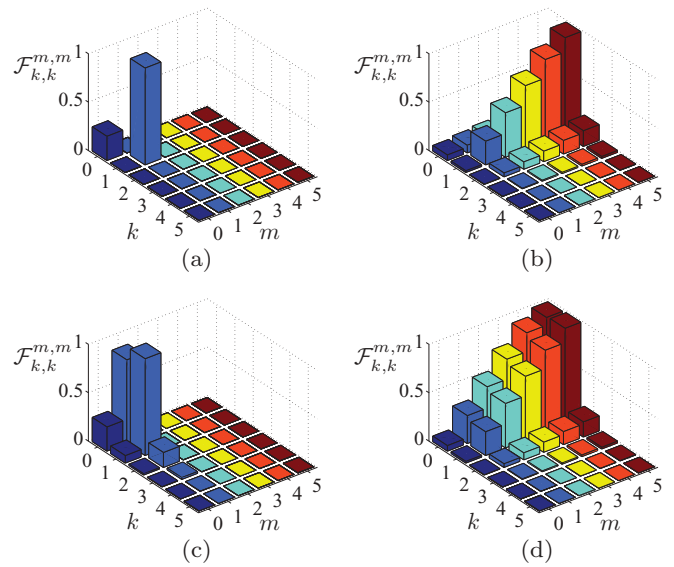

FIG. 3. (Color online) (a) Diagonal elements $\mathcal{F}_{k,k}^{m,m}$ of the ideal truncated noiseless amplifier process. (b) Diagonal elements $\mathcal{F}_{k,k}^{m,m}$ with nonunit detection efficiency of the APD D_1 ($\mu = 0.11$) and lack of photon-number resolution. (c) Diagonal elements $\mathcal{F}_{k,k}^{m,m}$ with nonideal generation of the single-photon state ($\delta = 1.089$). (d) Diagonal elements $\mathcal{F}_{k,k}^{m,m}$ including both experimental imperfections.

measurement consists of superposing the reflected portion of the single photon with the input state on a symmetric beam-splitter (S-BS) and performing photon counting at the outputs. Successful runs are heralded by the presence of a single photon on one output and the vacuum on the other. This operation produces an output state in the form $N(\alpha)(|0\rangle + g\alpha|1\rangle)$, where g is a gain factor determined by the reflexion R of the A-BS, $g = \sqrt{(1 - R)/R}$. For weak input intensities $\|\alpha\| \leqslant 0.1$, this truncated expansion is a good approximation of the amplified state $|g\alpha\rangle$. Figure 3(a) shows the elements $\mathcal{F}_{k,k}^{m,m}$ of the corresponding map, which would normally describe the population transfer among Fock states. In this case, instead, we notice the enhancement of the single-photon component and the suppression of all the higher-order terms. The complete process is a truncated form $\hat{C} = g^{\hat{n}}\Theta(\hat{n})$, where $\Theta(\hat{n})$ is 1 for $n \leqslant 1$ and zero otherwise.

Several departures from the ideal behavior prevent us from matching these simple predictions in the experiment, and a more refined description is then necessary. One of the main limitations is represented by single-photon detection. While the apparatus is quite robust against limited efficiency [19,33], it is nevertheless affected by the lack of photon-number resolution. The avalanche photodiode (APD) D_1, which heralds the successful events of the amplification process, will give a click each time that some light is absorbed, irrespective of the energy. This causes triggering events which do not originate from a single photon on D_1, which result in a transfer of population from higher-energy states to the one-photon Fock state, as it appears in Fig. 3(b), where the corresponding tensor is shown.

Single photons are produced by down-conversion in a nonlinear crystal: whenever an APD D_0 detects the presence of one photon, it heralds the twin photon on the correlated mode. The probabilistic nature of the emission allows for multiple-pair generation, which the APD is not able to

discriminate from single-pair events. The output state will not be a pure single photon, but will present contributions from higher-order terms. Furthermore, one needs to consider that the matching of the pump field with the observed modes will not be perfect. This results in excess noise in both the conditioning and signal modes, spoiling even more the quality of our single-photon state. This can be assessed in the experiment by measuring the quadrature distributions [12] and is described by the parameter δ [34,35], ranging from $\delta = 2$ for a pure heralded single-photon state to $\delta = 0$ for a thermal state. The effect on the process is illustrated in Fig. 3(c) showing how a higher-order number from multiple-pair emission can end up being populated.

Considering both imperfection sources provides an exhaustive model of our experiment: its accuracy, checked by calculating the fidelities between the experimental density matrices [19] and the prediction of the model, good enough, with an average figure of ~99.5% for weak intensities $\|\alpha\| \leqslant 1$ (right inset of Fig. 2), to use it for calculating the process map. The results, for the tensorial form, are summarized in Fig. 3(d): the two mechanisms take place independently and cause a lesser gain than expected and the presence of noise in the amplified states.

The transfer function can be decomposed in a correctly heralded one and a faulty one. For the correctly heralded transfer function, one could start with the beam-splitters: the asymmetric one is obtained by composing, with the use of Eq. (18), the beam-splitter transfer function with the Wigner function of the experimental single photon and the vacuum. In the same way, the transfer function for the part containing the S-BS is determined by composing the beam-splitter transfer function with the transfer function of the APD (Wigner function of the projection operator multiplied by 2π composed

with an attenuation transfer function) on one output and an attenuation (modelizing the mode-matching on one input) and then tracing on the remaining output mode. The final correctly heralded transfer function is obtained by composing those two transfer functions. The faulty transfer function is simply determined by composing an attenuation transfer function (taking into account the mode matching and the S-BS) with the APD transfer function.

While an inspection in the Fock basis can be informative, it does not lead to the most natural description of a process for continuous-variable states; also, from a practical point, it might be cumbersome to verify some properties such as the Gaussianity of the process or its nonclassicality from the expression of the $\mathcal{F}$ tensor. For this purpose, a useful approach consists of inspecting the trend of the associated transfer function: while this object generally acts on pairs of two-dimensional vectors, $\vec{r} = (x, p)$ and $\vec{r}' = (x', p')$, for phase-invariant processes—as is the case for the noiseless amplifier—the transfer function can only depend on $r = \sqrt{x^2 + p^2}$, $r' = \sqrt{x'^2 + p'^2}$, and $\theta = \cos^{-1}(\frac{\vec{r} \cdot \vec{r}'}{rr'})$. The transfer function for the noiseless amplifier is presented in Fig. 4, comparing the cases when an ideal single photon is used as an ancilla and with the actual resources. Nonclassical features are clear in the ideal limit with the negative values, especially around $r' = 0$. However, under experimental conditions, these

signatures are smoothed by the imperfections of the setup, though there remains a negative region. In more detail, we observe how low values of the transfer function for high r' correspond to the saturation of the amplifier, i.e., the impossibility of having more than one photon at the output. The negative peak determines the non-Gaussianity of the output states by causing a small negative region in the Wigner function of the output state; nevertheless, this feature vanishes rather quickly with the imperfection and is not visible in a realistic output state, as is shown in Fig. 4. Moreover, the slightly negative region around $r = 0$, which does not induce negativity in the Wigner function, remains even with the imperfections, leading to a more resilient negativity of the transfer function than the Wigner function of the output states. We can notice that the regions for small r and r' are quite different around $\theta = 0$ and $\theta = \pi$, this is due to the fact that the amplifier keeps the phase of the "small" states, whereas for bigger values of r and r' the transfer function is almost independent of θ since the higher photon-number terms in the input state often trigger the heralding, leading to a single photon (with losses) in the output state. A last remark concerns the increasing peak with r and the different scales between the two maps originating from the variation of the success probability.

V. EXAMPLE 2: PHOTON ADDITION

The extreme negative value of a Wigner function can be used as a quantifier of its nonclassicality [23]. However, an intuitive extension of such reasoning to the transfer functions would be severely affected by the probabilistic character of the process itself. Here we illustrate these considerations in a second example: the single-photon addition (which is an experimental approximation of $\hat{C} = \hat{a}^\dagger$). As above, our description is mediated by a model of the physical process.

In our implementation, photon addition is achieved by feeding the input state in an optical parametric amplifier (OPA) driven at low gain $g = \cosh^2 \chi$, where χ measures the nonlinear interaction strength and it is proportional to the pump intensity. To the first order, this process adds a photon
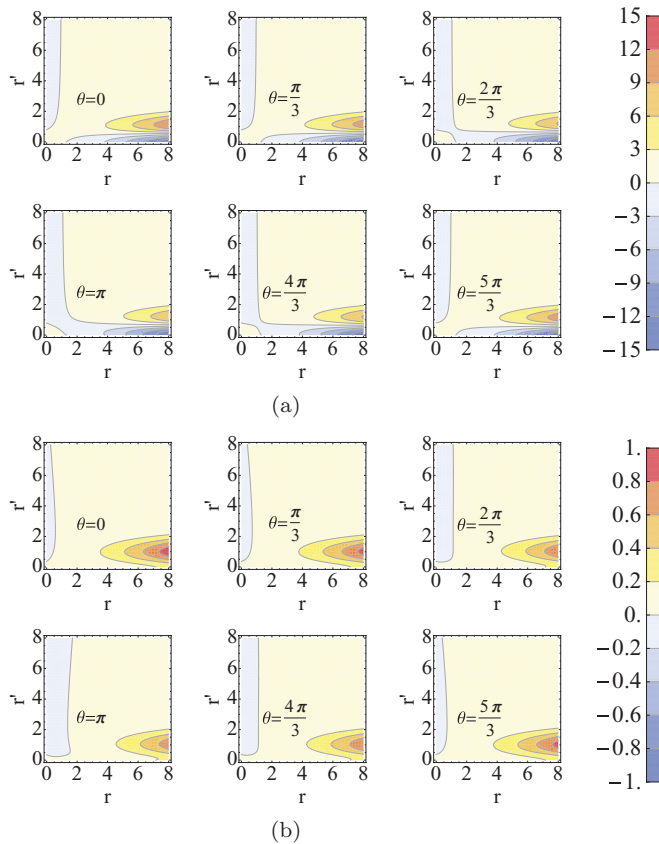

FIG. 4. (Color online) Contour plots of $f_{\mathcal{F}}(r', r, \theta)$ for the noise-less amplification process as a function of (r', r) for different values of θ. (a) Low APD detection efficiency μ and ideal generation of the single photon ($\delta = 2$). (b) Low APD detection efficiency μ and nonideal generation of the single photon ($\delta = 1.089$).
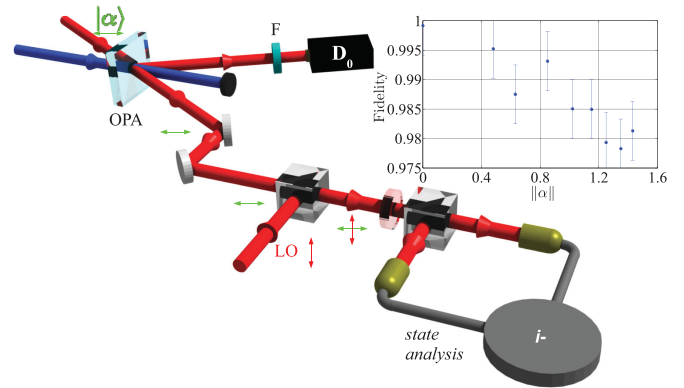

FIG. 5. (Color online) Layout of the single-photon addition experiment [23]. A single photon is conditionally added upon detection of a single photon on detector D_0. As above, the beam-splitters exploit polarization (double-sided arrows in the figure). Inset: Fidelities between the experimental density matrices [23] and the prediction of the model.
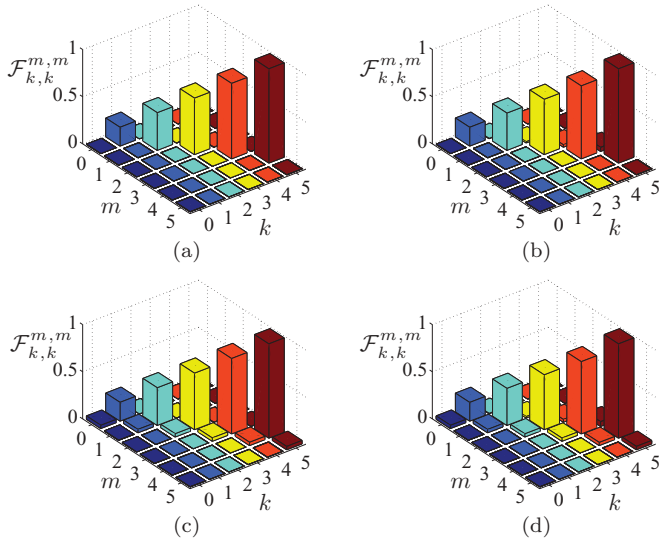
FIG. 6. (Color online) (a) Diagonal elements $\mathcal{F}_{k,k}^{m,m}$ of the ideal photon addition process. (b) Diagonal elements $\mathcal{F}_{k,k}^{m,m}$ for the case of a conditioned OPA driven at $\chi = 0.105$. (c) Diagonal elements $\mathcal{F}_{k,k}^{m,m}$ with a parasitic gain $\gamma = 0.425$ and very low gain. (d) Diagonal elements $\mathcal{F}_{k,k}^{m,m}$ including both experimental imperfections.

pair shared by the signal mode and a correlated mode, on which an APD D_0 is placed; due to the nondeterministc nature of the process, the successful events are triggered by a detection event from D_0 (Fig. 5). This method was introduced in Ref. [36] and then adopted for tests of the commutation rules [37,38] and the analysis of nonclassicality [39] and non-Gaussianity [23].

The main source of noise here can be identified in the imperfect matching between the pump and the signal modes, which results in a parasite gain $h = \cosh^2 \gamma \chi$. An estimate for these two gains, taken from a fit of their non-Gaussianity [23], is $\chi = 0.105$, and $\gamma = 0.425$ [23]. A third imperfection arises from the fact that spurious events might happen at D_0, due either to dark counts or to clicks originating from nonmatching modes. The fidelity between modeled and the reconstructed states using coherent states as inputs is satisfactory, although the data might be affected by some extra noise likely due to low-frequency fluctuations of the average level of the homodyne current.

As it appears from the comparison of Figs. 6(a) and 6(b), the gain χ is chosen to be sufficiently low so that two-pair events
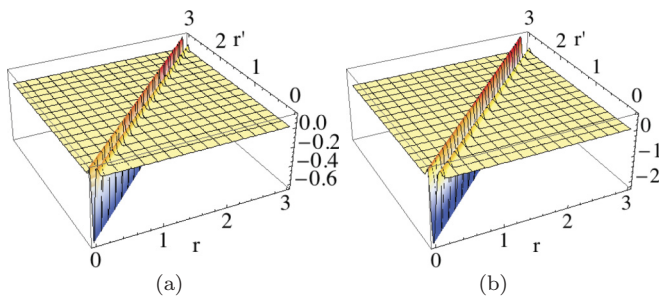

FIG. 7. (Color online) Plots of $f_{\mathcal{F}}(r',r,\theta)$ for the photon addition process as a function of (r',r) for $\theta = 0$. (a) With ideal OPA (driven at $\chi = 0.105$) and photon counter. (b) With a parasitic gain $\gamma = 0.425$ and an APD.
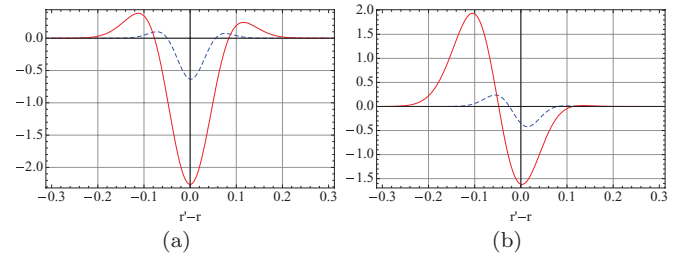

FIG. 8. (Color online) Plots of $f_{\mathcal{F}}(r',r,\theta)$ for the photon addition process as a function of $r' - r$. The plain line correspond to the experimental conditions ($\gamma = 0.425$ and an APD), and the dashed line to the ideal case. (a) For $\theta = 0$ and $r + r' = 2$. (b) For $\theta = 0$ and $r + r' = 20$.

are not significant: the transfer of population by more than one photon is low. On the other hand, the effect of the parasite gain seems as important: the sheer effect is the presence of uncorrelated clicks at D_0 that leave the state unchanged. This corresponds to the diagonal terms in Fig. 6(c), considered in the limit of extremely low gain $\chi \to 0$. The overall process simply results in the presence of these two imperfections. For the sake of simplicity we have only considered the case of low detection efficiency at D_0 [Fig. 6(d)]. In this example, the adoption of the quantum map formalism is revealed to be particularly clear and useful for the analysis of the process: not only does it confirm our intuition about the behavior of parasite processes but also it gives us a way of quantifying their effect in a way that does not depend on the particular input.

The correctly heralded transfer function is easy to determine: it is only a composition of the parametric downconversion transfer function with the Wigner function of vacuum on one input and the APD transfer function and attenuation transfer function on the outputs. As for the preceding example, we can use the radial symmetry of the process to express the transfer function in the simplest form $f_{\mathcal{F}}(r',r,\theta)$. In Fig. 7 we show the transfer function $f_{\mathcal{F}}(r',r,0)$ as a function of (r',r), as this contains much information about the physics: there we compare the case of low gain r and photon-number discrimination, and the full model of our experiment. For both cases, the transfer function has nonzero values only around $r' = r$ and for $\theta = 0$: this indicates that the amplitude and the phase are mostly unchanged by the process. The increase of the positive peak with the amplitude corresponds to the growth of the success rate with the number of photons and is more visible in the second graph because of the inability to discriminate the photon number. Finally, the negative peak introduces a negative part in the resulting Wigner function and is a sign of the non-Gaussianity of the process. We can note that the difference between the two scales (Fig. 8) is only due to the differences in the success rate, even for the negative peak. This implies that the size of the negative peak cannot be readily used to quantify the quantumness of a map.

VI. CONCLUSION

We have inspected two important processes for continuous-variable states with the formalism of quantum maps: these can convey interesting physical information about the process independently of the state. The adoption of a description in

terms of transfer functions offers a compact, insightful view of the process, along the same lines of what happens with the Wigner function for quantum states. We have applied this method to the description of the realistic operation of a noiseless amplifier and of a photon-adder, evidenciating how experimental imperfections shape the features of the transfer function.

[1] U. Leonhardt, *Measuring the Quantum State of Light* (Cambridge University Press, Cambridge, UK, 1998).

[2] D. F. V. James, P. G. Kwiat, W. J. Munro, and A. G. White, Phys. Rev. A **64**, 052312 (2001).

[3] J. L. O'Brien, G. J. Pryde, A. Gilchrist, D. F. V. James, N. K. Langford, T. C. Ralph, and A. G. White, Phys. Rev. Lett. **93**, 080502 (2004).

[4] M. Lobino, D. Korystov, C. Kupchak, E. Figueroa, B. C. Sanders, and A. I. Lvovsky, Science **322**, 563 (2008).

[5] J. S. Lundeen, A. Feito, H. Coldenstrodt-Ronge, K. L. Pregnell, C. Silberhorn, T. C. Ralph, J. Eisert, M. B. Plenio, and I. A. Walmsley, Nat. Phys. **5**, 27 (2008).

[6] K. Kraus, *States, Effects and Operations: Fundamental Notions of Quantum Theory* (Academic Press, San Diego, 1983).

[7] M. G. A. Paris, M. Cola, and R. Bonifacio, Phys. Rev. A **67**, 042104 (2003).

[8] B. P. Lanyon, M. Barbieri, M. P. Almeida, T. Jennewein, T. C. Ralph, K. J. Resch, G. J. Pryde, J. L. O'Brien, A. Gilchrist, and A. G. White, Nat. Phys. **5**, 134 (2008).

[9] A. I. Lvovsky, H. Hansen, T. Aichele, O. Benson, J. Mlynek, and S. Schiller, Phys. Rev. Lett. **87**, 050402 (2001).

[10] J. Wenger, R. Tualle-Brouri, and P. Grangier, Phys. Rev. Lett. **92**, 153601 (2004).

[11] A. Zavatta, S. Viciani, and M. Bellini, Phys. Rev. A **70**, 053821 (2004).

[12] A. Ourjoumtsev, R. Tualle-Brouri, J. Laurat, and P. Grangier, Science **312**, 83 (2006).

[13] A. Ourjoumtsev, H. Jeong, R. Tualle-Brouri, and P. Grangier, Nature (London) **448**, 784 (2007).

[14] J. Eisert, S. Scheel, and M. B. Plenio, Phys. Rev. Lett. **89**, 137903 (2002).

[15] J. Fiurasek, Phys. Rev. Lett. **89**, 137904 (2002).

[16] J. Niset, J. Fiurasek, and N. J. Cerf, Phys. Rev. Lett. **102**, 120501 (2009).

[17] A. Ourjoumtsev, A. Dantan, R. Tualle-Brouri, and P. Grangier, Phys. Rev. Lett. **98**, 030502 (2007).

[18] H. Takahashi, J. S. Neergaard-Nielsen, M. Takeuchi, M. Takeoka, K. Hayasaka, A. Furusawa, and M. Sasaki, Nat. Photonics **4**, 178 (2010).

[19] F. Ferreyrol, M. Barbieri, R. Blandino, S. Fossier, R. Tualle-Brouri, and P. Grangier, Phys. Rev. Lett. **104**, 123603 (2010).

[20] G. Y. Xiang, T. C. Ralph, A. P. Lund, N. Walk, and G. J. Pryde, Nat. Photonics **4**, 316 (2010).

[21] N. Kiesel, C. Schmid, U. Weber, R. Ursin, and H. Weinfurter, Phys. Rev. Lett. **95**, 210505 (2005).

[22] I. Bongioanni, L. Sansoni, F. Sciarrino, G. Vallone, and P. Mataloni, Phys. Rev. A **82**, 042307 (2010).

[23] M. Barbieri, N. Spagnolo, M. G. Genoni, F. Ferreyrol, R. Blandino, M. G. A. Paris, P. Grangier, and R. Tualle-Brouri, Phys. Rev. A **82**, 063833 (2010).

[24] M. Nielsen and I. Chuang, *Quantum Computation and Quantum Information*, Cambridge Series on Information and the Natural Sciences (Cambridge University Press, Cambridge, UK, 2000).

[25] M. Berry, N. Balazs, M. Tabor, and A. Voros, Ann. Phys. **122**, 26 (1979).

[26] C. Cohen-Tannoudji, Lecture Notes of Collège de France, available at http://www.phys.ens.fr/cours/college-de-france/1983-84/1983-84.htm.

[27] C. Gardiner and P. Zoller, *Quantum Noise: A Handbook of Markovian and Non-Markovian Quantum Stochastic Methods with Applications to Quantum Optics*, Springer Series in Synergetics (Springer, New York, 2004).

[28] K. Blum, *Density Matrix Theory and Applications*, Atomic, Optical, and Plasma Physics (Springer, New York, 2012).

[29] I. Bengtsson and K. Zyczkowski, *Geometry of Quantum States: An Introduction to Quantum Entanglement* (Cambridge University Press, Cambridge, UK, 2006).

[30] C. Ferrie and J. Emerson, J. Phys. A **41**, 352001 (2008).

[31] R. W. Spekkens, Phys. Rev. Lett. **101**, 020401 (2008).

[32] S. Rahimi-Keshari, A. Scherer, A. Mann, A. T. Rezakhani, A. I. Lvovsky, and B. C. Sanders, New J. Phys. **13**, 013006 (2011).

[33] T. C. Ralph and A. P. Lund, in *Quantum Communication Measurement and Computing Proceedings of 9th International Conference*, AIP Conference Proceedings Vol. 1110, edited by A. I. Lvovsky (American Institute of Physics, New York, 2009), p. 155.

[34] A. Ourjoumtsev, R. Tualle-Brouri, and P. Grangier, Phys. Rev. Lett. **96**, 213601 (2006).

[35] F. Ferreyrol, R. Blandino, M. Barbieri, R. Tualle-Brouri, and P. Grangier, Phys. Rev. A **83**, 063801 (2011).

[36] A. Zavatta, S. Viciani, and M. Bellini, Phys. Rev. A **72**, 023820 (2005).

[37] V. Parigi, A. Zavatta, M. S. Kim, and M. Bellini, Science **317**, 1890 (2007).

[38] A. Zavatta, V. Parigi, M. S. Kim, H. Jeong, and M. Bellini, Phys. Rev. Lett. **103**, 140406 (2009).

[39] A. Zavatta, V. Parigi, and M. Bellini, Phys. Rev. A **75**, 052106 (2007).